

Carcinogenesis in Mouse Stomach by Simultaneous Activation of the Wnt Signaling and Prostaglandin E2 Pathway

メタデータ	言語: eng 出版者: 公開日: 2017-10-05 キーワード (Ja): キーワード (En): 作成者: メールアドレス: 所属:
URL	http://hdl.handle.net/2297/2853

Carcinogenesis in mouse stomach by simultaneous activation of the Wnt signaling and prostaglandin E₂ pathway

Hiroko Oshima^{*,‡}, Akihiro Matsunaga[‡], Takashi Fujimura[§], Tetsuya Tsukamoto[¶], Makoto M. Taketo[‡], and Masanobu Oshima^{*,‡}

*Division of Genetics, Cancer Research Institute, Kanazawa University, Kanazawa Japan; [‡]Department of Pharmacology, Kyoto University Graduate School of Medicine, Kyoto, Japan; [§]Gastroenterologic Surgery, Kanazawa University Hospital, Kanazawa, Japan; [¶]Division of Oncological Pathology, Aichi Cancer Center Research Institute, Nagoya, Japan

Grant Support:

Supported by Grants-in-Aid for Scientific Research from the Ministry of Education, Culture, Sports, Science and Technology of Japan to H.O., M.M.T. and M.O., and the Uehara Memorial Foundation to H.O.

The authors thank Manami Watanabe for technical assistance.

Short Title: Wnt and PGE₂ in gastric carcinogenesis

Correspondence:

Masanobu Oshima, D.V.M., Ph.D.,
Division of Genetics, Cancer Research Institute, Kanazawa University,
13-1 Takara-machi, Kanazawa, 920-0934 Japan.
Phone: +81-76-265-2721, FAX: +81-76-234-4519
e-mail: oshimam@kenroku.kanazawa-u.ac.jp

Abbreviations used in this paper: APC, adenomatous polyposis coli; BrdU, bromodexyuridine; COX-2, cyclooxygenase-2; mPGES-1, microsomal prostaglandin

E synthase-1; MVD, microvessel density; PGE₂, prostaglandin E₂; PPAR δ , Peroxisome proliferator-activated receptor δ ; RT-PCR, reverse-transcribed polymerase chain reaction; SPEM, spasmolytic polypeptide (TFF2)-expressing metaplasia; TFF2, trefoil factor 2; vWF, von Willebrand Factor.

Abstract

Background & Aims: Accumulating evidence indicate that prostaglandin E₂ (PGE₂), a downstream product of cyclooxygenase 2 (COX-2), plays a key role in gastric tumorigenesis. The Wnt pathway is also suggested to play a causal role in gastric carcinogenesis. However, the molecular mechanism remains poorly understood how the Wnt and PGE₂ pathways contribute to gastric tumorigenesis. To investigate the role of Wnt and PGE₂ in gastric cancer, we have generated transgenic mice that activate both pathways, and examined their phenotypes. **Methods:** We constructed *K19-Wnt1* transgenic mice expressing *Wnt1* in the gastric mucosa using the keratin 19 promoter. We then crossed *K19-Wnt1* mice with another transgenic line *K19-C2mE* to obtain *K19-Wnt1/C2mE* compound transgenic mice. The *K19-C2mE* mice express COX-2 and microsomal prostaglandin E synthase-1 (mPGES-1) in the stomach, showing an increased gastric PGE₂ level. We examined the gastric phenotypes of both *K19-Wnt1* and *K19-Wnt1/C2mE* mice. **Results:** *K19-Wnt1* mice had a significant suppression of epithelial differentiation, and developed small preneoplastic lesions consisting of undifferentiated epithelial cells with macrophage accumulation. Importantly, additional expression of COX-2 and mPGES-1 converted the preneoplastic lesions in the *K19-Wnt1* mice into dysplastic gastric tumors by 20 weeks of age. Notably, we found mucous cell metaplasia in the glandular stomach of the *K19-Wnt1/C2mE* mice as early as 5 weeks of age, before

the dysplastic tumor development. Conclusions: Wnt signaling keeps the gastric progenitor cells undifferentiated. Simultaneous activation of both Wnt and PGE₂ pathways causes dysplastic gastric tumors through the metaplasia-carcinoma sequence.

Introduction

The binding of Wnt ligands to a Frizzled receptor destabilizes the β -catenin degradation complex containing APC, thereby allowing the nuclear translocation of β -catenin followed by transcriptional activation of the Wnt target genes¹. The constitutive activation of the Wnt pathway by mutations in either the *Apc* or β -catenin gene results in intestinal polyposis^{2,3}. Nuclear localization of β -catenin, a hallmark of Wnt activation, is found also in about 30% of gastric cancer tissues⁴, suggesting that Wnt pathway activation is one of the major causes of gastric carcinogenesis. However, there is few genetic evidence for Wnt activation in gastric cancer.

Epidemiological evidence shows that *Helicobacter pylori* infection is associated with gastric cancer⁵. We recently demonstrated that an infection of mice with *Helicobacter felis*, a close relative of *H. pylori*, induces expression of both cyclooxygenase-2 (COX-2) and microsomal prostaglandin E synthase-1 (mPGES-1) in the gastric mucosa⁶. Inducible enzyme COX-2 catalyzes biosynthesis of prostaglandin (PG)H₂, which is further converted to PGE₂ by mPGES-1⁷. Expression of both COX-2 and mPGES-1 is also induced in a variety of cancer tissues⁸. It is established that COX-2 plays a key role in gastrointestinal cancer development⁹, and inhibition of COX-2 in mouse models by selective inhibitors suppresses gastric and intestinal tumorigenesis^{10,11}. Furthermore, PGE₂ is also implicated in gastrointestinal tumor development^{12,13}. Accordingly, it is essential for gastric tumorigenesis to increase the level of PGE₂ through induction of COX-2 and mPGES-1.

However, the cooperation of Wnt signaling and the PGE₂ pathway has not yet been investigated in gastric tumorigenesis. In this study, we have constructed transgenic mice expressing *Wnt1* in the gastric mucosa, and examined epithelial proliferation and differentiation. We then introduced COX-2 and mPGES-1 genes into the *Wnt1* transgenic mice by crossing with the other transgenic line, and studied the changes in the gastric lesions.

Materials and Methods

Tissue samples

In total, 80 patients were pre-operatively diagnosed with sporadic gastric cancer (47 intestinal-type and 33 diffuse type) in 1998-1999 at Kanazawa University Hospital, Japan. Any patients with signet ring cell carcinoma were excluded because of the difficulty in evaluating nuclear β -catenin staining. All experiments were carried out according to the protocol approved by the Ethics Committee of Kanazawa University. Informed consent was obtained from all participants.

Transgenic mice

The K19 promoter with a synthetic intron and SV40 poly(A) cassette were described previously⁶. Although the K19 promoter used in the present study is transcriptionally active in the gastric epithelium, its expression spectrum in the whole body is slightly different from the endogenous K19 gene possibly caused by the limited length of the promoter fragment⁶. *Wnt1* cDNA was excised from pUSEamp-Wnt1 (Upstate, Charlottesville, VA). These fragments were cloned into pBluescript (Stratagene, La Jolla, CA) to construct the pK19-Wnt1 transgenic vector. The expression vector was microinjected into the fertilized eggs of F1 (C3H and C57BL/6) hybrid females crossed with C57BL/6 males to generate *K19-Wnt1* transgenic mice. Expression of *Wnt1* in the gastric mucosa was confirmed by RT-PCR. Construction of *K19-C2mE* transgenic mice has been described previously⁶. To minimize any genetic background differences, we used littermate mice for the experiments

from the mating of N2-backcrossed *K19-Wnt1* with N6-backcrossed *K19-C2mE* mice. Backcrossing was performed using wild-type C57BL/6 mice. Construction of *Ap^c^{A716}* mice has been previously described². All animal experiments were carried out according to the protocol approved by the Ethics Committees on Animal Experimentation of Kyoto University and Kanazawa University.

Histology and immunohistochemistry

Tissues were fixed in 4% paraformaldehyde, embedded and sectioned at 4- μ m thickness. Sections were stained with H&E or Alcian blue at pH 2.5. To detect nuclear β -catenin, mouse monoclonal antibody for the stabilized (active) form of β -catenin (Clone 8E7, Upstate, Charlottesville, VA) was used as the primary antibody after autoclaving the sections for 20 min in sodium citrate buffer (pH 6.0). This antibody is specific for the active form of human and mouse β -catenin, dephosphorylated on Ser37 or Thr41. To detect total β -catenin, polyclonal anti- β -catenin antibody (Sigma, St. Louis, MO) was used. This antibody reacts with human and mouse β -catenin peptide corresponding to amino acids 768-781. For the cell proliferation analysis, monoclonal rat anti-mouse Ki-67 antibody (Clone TEC-3, DakoCytomation, Carpinteria, CA) was used. This antibody is specific for the mouse Ki-67, a nuclear protein expressed during all phases of the cell cycle (G_1 , S, G_2 and M phases). To detect macrophages, rat monoclonal anti-mouse F4/80 antibody (MCA497R; Clone A3-1, Serotec, Oxford, UK) was used. This antibody recognizes the mouse F4/80 antigen expressed by macrophages. To detect capillary vessels, polyclonal anti-von

Willebrand Factor (vWF) antibody (DakoCytomation, Carpinteria, CA) was used. This antibody reacts with endothelial cells. The MOM Kit (Vector Laboratories, Burlingame, CA) was used to minimize the background staining signals. Staining signals were visualized using the Vectorstain Elite Kit (Vector Laboratories, Burlingame, CA).

BrdU labeling index

Mice were injected *i.p.* with 200 μ l of BrdU solution (BD Pharmingen, San Diego, CA) at 30 min before euthanasia. Tissue samples were fixed in 4% paraformaldehyde, embedded and sectioned at 4- μ m thickness. These sections were stained with anti-BrdU antibody (BD Pharmingen). The number of BrdU-positive cells per gland (Fig. 3E) or microscopic field (Fig. 8) was calculated as the BrdU labeling index. BrdU positive cells were counted in 5 high-powered fields.

In situ hybridization

Rehydrated paraffin sections were digested with 5 μ g/ml of proteinase K, hybridized overnight with 500 ng/ml of riboprobe, and then were stringently washed in $2 \times$ SSC/50% formamide, followed by $0.1 \times$ SSC. The anti-sense and sense riboprobes were labeled using digoxigenin-labeling reagent (Roche Diagnostics, Indianapolis, IN). The sense probe was used as a negative control (data not shown).

Scoring Preneoplastic Lesions

After fixation with 4% paraformaldehyde for 20 min, stomach tissue were stained with 0.05% toluidine blue solution for 30 min, and then the total number of preneoplastic

lesions in the glandular stomach were scored using a dissecting microscope.

Scoring Microvessel Density (MVD).

MVD was determined using histological sections immunostained with anti-vWF antibody. The microscopic field that contained the highest number of capillaries was chosen for each sample by an initial scan at a low-magnification ($\times 100$). Then, the vessels were counted in high-magnification fields ($\times 400$). At least, 5 microscopic fields for each genotype were scored. Relative MVD was calculated by dividing the mean number of each MVD with the mean value of the wild-type MVD.

Immunoblotting Analysis

The tissue samples were homogenized and sonicated in lysis buffer. After centrifugation at $2,000 \times g$, 10 μg of the supernatant protein was separated in a 10% SDS-polyacrylamide gel. Antibodies for unphosphorylated β -catenin (Upstate, Charlottesville, VA), total β -catenin (Sigma, St. Louis, MO), and COX-2 (Cayman Chemical, Ann Arbor, MI) were used as the primary antibody. The ECL detection system (Amersham Biosciences, Buckinghamshire, UK) was used to detect the specific signals.

Statistical Analysis

Data were analyzed by the unpaired *t*-test using Microsoft Excel 2004 (Microsoft), and presented as the mean \pm standard deviation (s.d.). A value of $P < 0.05$ was accepted as statistically significant.

Results

Activation of the Wnt Pathway in Human Gastric Cancer Tissues

We first examined 80 cases of gastric cancer (47 and 33 cases for the intestinal type and diffuse type, respectively) by immunohistochemistry (Figure 1). The nuclear localization of β -catenin was detected in 24 and 19 cases of intestinal-type and diffuse type gastric cancer, respectively, whereas β -catenin was found in the basolateral membrane of the adjacent normal tissues of the same patients (Figure 1B, C, E and F). These results suggest that the Wnt pathway is activated in 54% of the gastric cancer tissues examined (Figure 1G), and that Wnt signaling plays a causal role in gastric carcinogenesis.

Construction of *K19-Wnt1* Transgenic Mice

To further investigate the genetic mechanism of Wnt signal activation in gastric carcinogenesis, we constructed transgenic mice (*K19-Wnt1*) that express *Wnt1* in the gastric epithelial cells using cytokeratin19 (K19) gene promoter (Figure 2A). We used the *Wnt1* cDNA for transgenic expression because *Wnt1* is one of the Wnt ligands in the canonical Wnt pathway. We confirmed the expression of *Wnt1* in the constructed *K19-Wnt1* mouse stomach by RT-PCR (Figure 2B), although *Wnt1* was not detected in the wild-type gastric mucosa. The levels of unphosphorylated (active form) β -catenin increased significantly in the *Wnt1* transgenic mice (lines #1 through #5) compared with that in the wild-type mice (Figure 2C), indicating activation of the canonical Wnt pathway in the transgenic mouse gastric mucosa. Notably, the level of unphosphorylated β -catenin in the *K19-Wnt1* mice (lines #1 and #2) was

similar to that in *Apc*^{A716} mouse intestinal polyps where the canonical Wnt pathway was activated by the loss of the wild-type *Apc* gene². Because these two transgenic lines, #1 and #2, showed essentially the same phenotypes, we present here the results of line #2 (hereafter called: *K19-Wnt1*).

Suppression of Gastric Epithelial Differentiation by Wnt Activation

Given that Wnt signaling is essential for maintaining the intestinal crypt that contains epithelial progenitor cells and stem cells^{14,15}, we examined gastric epithelial differentiation in the *K19-Wnt1* mice. The trefoil factor 2 (TFF2) was used as an undifferentiated epithelial marker, because it was detected in the small isthmal cells (Figure 3A and B) where β -catenin accumulated in both the nucleus and cytoplasm (Figure 3C). Among these small isthmal cells, gastric progenitor cells and granule-free stem cells exist¹⁶. Notably, we found that the TFF2-expressing cell population expanded to the upper gland in the *K19-Wnt1* mouse stomach, although it was limited to the isthmus in the wild type (Figure 3D). The number of TFF2-positive cells was twice as high in the *K19-Wnt1* mice as in the wild-type mice. Moreover, the number of BrdU incorporating cells with 30-minute labeling was 1.6-fold higher in the *K19-Wnt1* gastric mucosa than in wild type (Figure 3E). Most BrdU-labeled cells within 30 minutes are considered to be gastric progenitor cells¹⁶. Consistently, the *K19-Wnt1* mice contained 1.5 times more Ki-67-positive cells than the wild type (Figure 3F). These results indicate that Wnt signaling activation causes expansion of the undifferentiated progenitor cell population in the glandular stomach.

Preneoplastic Lesions in the *K19-Wnt1* Mouse Glandular Stomach

In the glandular stomach of the *K19-Wnt1* mice, we found limited numbers of small lesions from 7 weeks of age as thickened mucosal foci under a dissecting microscope (Figure 4B). The mean number of 37 such lesions in the whole glandular stomach at 18 weeks of age was significantly higher than 4.5 at 7 weeks (n=3 for each age), whereas no such lesions existed in the wild-type mice (Figure 4A and C). Histologically, the lesion contained undifferentiated epithelium consisting of small isthmal cells with irregular branching (Figure 4D). We found increased proliferation rates of epithelial cells by Ki-67 immunostaining (Figure 4E), and β -catenin accumulation in the undifferentiated epithelial cells (Figure 4F). Accordingly, these preneoplastic lesions consisted of Wnt-activated epithelial cells.

Dysplastic Gastric Tumors Caused by the Cooperation of the Wnt and PGE₂ Pathways

We then examined whether PGE₂ produced by the activation of COX-2 and mPGES-1 contributes to Wnt-dependent gastric carcinogenesis. We crossed *K19-Wnt1* mice with another transgenic line (*K19-C2mE*⁶) that expresses both COX-2 and mPGES-1 in the gastric mucosa, and generated compound transgenic line *K19-Wnt1/C2mE*. We confirmed large amounts of COX-2 protein in the stomach of both *K19-C2mE* and *K19-Wnt1/C2mE* mice (Figure 2D) and lack of *Wnt1* expression in the *K19-C2mE* gastric mucosa (Figure 2B). Notably, *Wnt1* expression in the *K19-Wnt1/C2mE* mouse stomach increased significantly compared with that in the *K19-Wnt1* mice (Figure 2B). This may be caused by increased

number of *Wnt1*-expressing undifferentiated cells in the *K19-Wnt1/C2mE* stomach (see below). Importantly, we found large tumors associated with hyperemia in the *K19-Wnt1/C2mE* mice at 30 weeks of age (Figure 5B). No such tumors were found in either *K19-Wnt1* or *K19-C2mE* mice (Figure 5C and D), although mucosal hyperplasia developed in the *K19-C2mE* mice in the proximal glandular stomach as we reported previously⁶ (Figure 5D). The hyperplasia in the *K19-C2mE* mice consisted of the TFF2-expressing metaplastic mucous cells, *i.e.*, spasmolytic polypeptide (TFF2)-expressing metaplasia (SPEM)¹⁷.

Histologically, the gastric tumors in the *K19-Wnt1/C2mE* mice consisted of dysplastic epithelial cells with nuclear stratification and irregularly branched tubules (Figure 5B and E). The tumor epithelial cells had nuclear accumulation of β -catenin (Figure 5F). We also found increased Ki-67 labeling, indicating an increased proliferation of tumor cells (Figure 5G). These histological characteristics resembled those of human intestinal-type gastric cancer (Figure 1A and B). Furthermore, we found TFF2-expressing SPEM also adjacent to the dysplastic tumor tissue of the *K19-Wnt1/C2mE* mice (Figure 5H), showing a similar histology to human gastric adenocarcinoma¹⁸. Tumor invasion into the smooth muscle layers were also found in the 50, 75 and 100% of the *K19-Wnt1/C2mE* mice at 20, 30 and 50 weeks of age, respectively (Figure 5I and J). The incidence of dysplastic gastric tumors was 100% in the *K19-Wnt1/C2mE* mice older than 20 weeks of age (Figure 5K). Five of them became moribund between 25 and 50 weeks of age (data not shown). These results collectively indicate that the simultaneous activation of the Wnt and PGE₂ pathways causes

development of dysplastic gastric tumors by their synergistic effects. We did not find any metastatic tumors in other tissues including lymph nodes, liver, lung and peritoneum.

Macrophage Accumulation in Dysplastic Tumors and Preneoplastic Lesions

Tissue macrophages are implicated in the proliferation of epithelial progenitor cells in the intestine¹⁹. We thus examined macrophage infiltration in the respective mutant mice by immunostaining. We found abundant macrophages in the large gastric tumors of the *K19-Wnt1/C2mE* mice, whereas tissue macrophages were sparsely scattered in the wild-type glandular stomach (Figure 6A and B). This is consistent with the previous results that macrophages are accumulated in the gastric mucosa of the simple *K19-C2mE* transgenic mice, probably caused by increased PGE₂ and chemokine signaling⁶. It is worth noting that macrophages accumulated also in the small preneoplastic lesions of the *K19-Wnt1* mice (Figure 6C). These results suggest that macrophages play an important role in the Wnt-dependent preneoplastic and neoplastic changes, possibly through secreting growth factors and cytokines like tumor associated macrophages²⁰.

Increased Angiogenesis in the *K19-Wnt1/C2mE* Tumors

We have previously shown that PGE₂ signaling is important for angiogenesis in the intestinal tumorigenesis²¹. We thus examined angiogenesis in the *K19-Wnt1* and *K19-Wnt1/C2mE* mouse stomach by immunostaining using an anti-vWF antibody, and determined relative microvessel density (MVD). Although MVD in the *K19-Wnt1* gastric mucosa stayed at the same level as that in the wild-type mice, it increased significantly in the

K19-Wnt1/C2mE tumors (Figure 6D-F). Accordingly, it is possible that PGE₂ signaling contributes to gastric tumor development through stimulation of angiogenesis as well as macrophage recruitment in the Wnt-activated gastric mucosa.

Gastric Tumorigenesis through Metaplasia-Carcinoma Sequence in

K19-Wnt1/C2mE Mice

To understand the histopathogenesis of gastric tumor development, we examined the *K19-Wnt1/C2mE* and *K19-C2mE* mice chronologically at 5, 10, 20 and 50 weeks of age (Figure 7A-P). The *K19-Wnt1/C2mE* mice showed mucous metaplasia with Alcian-blue positive cells at 5 weeks of age, the same phenotype as in the *K19-C2mE* mice (Figure 7A, E, I and M). In the wild-type mouse gastric mucosa, weak Alcian-blue staining was detected only in the mucous neck cells (Figure 7E right). We also found dysplastic tumor cells (Alcian blue negative) in the metaplastic lesion of the *K19-Wnt1/C2mE*, but not in the *K19-C2mE* mice at 10 weeks of age (Figure 7B, F, J and N). The number of the dysplastic cells increased with age, and the mucous cells were found adjacent to the dysplastic tumors at 20 weeks of age (Figure 7C and G). These histological characteristics were consistent with the finding that SPEM was found adjacent to the dysplastic tumors at 30 weeks of age (Figure 5H). By 50 weeks of age, dysplastic tumor cells predominated the tumors of the *K19-Wnt1/C2mE* mice (Figure 7D and H). In contrast, no dysplastic signs were found in the *K19-C2mE* mice even at 50 weeks of age (Figure 7L and P). These results indicate that the increased PGE₂ level caused epithelial metaplasia to the SPEM lineage, and that simultaneous activation of

the Wnt and PGE₂ pathways causes development of dysplastic gastric tumors through metaplasia stage.

Increased Proliferation by the Activation of Wnt and PGE₂ Pathways

We next determined the proliferation rates of normal and tumor epithelial cells by BrdU incorporation assays (Figure 8). The BrdU labeling index in the stomach of both *K19-Wnt1/C2mE* and *K19-C2mE* mice was stomach significantly higher than in the wild-type mice from 5 weeks of age. Thus, increased PGE₂ signaling appears to be responsible for the hyperproliferation of gastric epithelial cells. Furthermore, *K19-Wnt1/C2mE* mice showed even higher labeling index than the *K19-C2mE* mice after 20 weeks of age, suggesting that simultaneous activation of both Wnt and PGE₂ pathways may thus lead the epithelial cells to further epithelial cell proliferation. This interpretation is consistent with the increased number of proliferating dysplastic cells in the *K19-Wnt1/C2mE* stomach.

Discussion

Wnt signaling plays an important role in the maintenance of the intestinal crypt containing the stem cells and undifferentiated progenitor cells^{14,15}. In the gastric gland, Wnt signaling also keeps the progenitor cells undifferentiated in the isthmus of the gastric gland, as we have shown that the number of progenitors increased significantly in the *K19-Wnt1* mouse stomach. It has been reported that Wnt signal activation was found in 30% of the human gastric cancer examined⁴. In the present study, we have found nuclear accumulation of β -catenin in 54% of the gastric cancer tissues examined. The high frequency of Wnt signal activation is likely due to the improved staining method and use of the specific antibody for the unphosphorylated and therefore stabilized form of β -catenin (see Materials and Methods). Accordingly, our results suggest that Wnt signaling is one of the major causes of gastric carcinogenesis regardless of the histological type. On the other hand, the COX-2 pathway has been demonstrated to play a key role in a variety of cancers including gastric tumorigenesis⁹⁻¹³. Therefore, it is possible that both Wnt signaling and the COX-2 pathway are activated simultaneously in some human gastric cancers. We have presented genetic evidence for such simultaneous activation of the Wnt and PGE₂ pathways in gastric carcinogenesis. On the other hand, we did not find any preneoplastic lesions or tumors in the stomach of the *Apc*^{A716} mice that is a model for familial adenomatous polyposis (data not shown). In the *Apc*^{A716} mice, somatic loss of the wild-type *Apc* gene is required for Wnt activation², whereas Wnt1 is constitutively expressed in the *K19-Wnt1/C2mE* mouse

stomach. Accordingly, it is possible that the frequency of simultaneous induction of both Wnt and PGE₂ pathways is considerably low in the *Apc*^{A716} mouse gastric mucosa, and this may explain the absence of gastric tumors.

Epidemiologic evidence indicates that *Helicobacter pylori* infection contributes to gastric carcinogenesis⁵. We recently demonstrated that infection of mice with *H. felis*, a close relative of *H. pylori*, induces both COX-2 and mPGES-1 in the gastric mucosa, raising the PGE₂ level as in the *K19-C2mE* mice⁶. Accordingly, it is possible that Wnt activation through a mutation in *APC* or β -catenin in the *H. pylori*-infected stomach imposes an increased risk of gastric carcinogenesis by the synergistic effects of the Wnt and PGE₂ pathways.

We previously showed that an increased PGE₂ level by simultaneous expression of COX-2 and mPGES-1 causes gastric hyperplasia with mucous cell metaplasia to the SPEM lineage¹⁷. Gastric metaplasia to the SPEM lineage has a strong association with human gastric adenocarcinoma and is considered as a precursor of gastric cancer^{18,22}. As anticipated, the *K19-Wnt1/C2mE* mice developed mucous metaplasia at 5 weeks of age with a similar histology to SPEM in the *K19-C2mE* mice. Importantly, we found dysplastic tumor cells in the metaplastic lesions in 10- to 30-week-old mice, respectively, with the SPEM adjacent to the dysplastic tumors. These results are consistent with the interpretation that dysplastic gastric tumors are derived from the SPEM by activation of both the Wnt and PGE₂ pathways. Therefore, the *K19-Wnt1/C2mE* model can be a useful tool to study molecular pathogenesis

of the gastric cancer through metaplasia-carcinoma sequence.

We found accumulated macrophages in the preneoplastic lesion of the *K19-Wnt1* mice. Tissue macrophages are important component of intestinal progenitor niche¹⁹. Moreover, tumor associated macrophages play an important role in tumor growth through secretion of cytokines, chemokines and growth factors²⁰. Consistently, we have shown that accumulation and activation of macrophages in the *K19-C2mE* mouse stomach are responsible for gastric metaplasia and hyperplasia^{6,17}. Accordingly, it is possible that accumulated macrophages cooperate with Wnt pathway activation in the development of preneoplastic lesions in the *K19-Wnt1* mice. The molecular mechanisms that recruit macrophages remain to be investigated further. We have previously reported that PGE₂-dependent angiogenesis is one of the key factors for intestinal polyp development²¹. Here, we found that angiogenesis is also stimulated in the *K19-Wnt1/C2mE* tumors. Accordingly, it is possible that PGE₂ signaling contributes gastric tumorigenesis through angiogenesis as well as macrophage activation.

Recently, crosstalk has been reported between Wnt signaling and COX-2 pathway²³. Peroxisome proliferator-activated receptor δ (PPAR δ) is one of the Wnt target genes. The PGE₂ signaling accelerates growth of intestinal adenomas, which is suppressed by inhibition of PPAR δ . These results suggest that PPAR δ is a focal point of the crosstalk between the Wnt and PGE₂ pathways. Another line of evidence shows that PGE₂ signaling through EP2 receptor releases GSK-3 β from β -catenin degradation complex and phosphorylates GSK-3 β

through activation of PI3K/Akt²⁴. Consequently, β -catenin is stabilized, and Wnt signaling is activated. To further investigate the molecular changes responsible for the crosstalk between Wnt and PGE₂ signaling, we examined the microarray expression profiles in the glandular stomach of the *K19-C2mE* and wild-type mice (GEO database; accession number, GSE3903). Because *K19-Wnt1/C2mE* mice but not *K19-Wnt1* mice develop gastric tumors, we expect that some of the upregulated molecules in the *K19-C2mE* mice are such candidates, and possible new targets for the prevention and treatment of gastric cancer.

In conclusion, simultaneous activation of the Wnt signaling and PGE₂ pathway can cause gastric carcinogenesis. Our compound transgenic mouse strain *K19-Wnt1/C2mE* is a genetic model for gastric carcinogenesis in the metaplasia-carcinoma sequence, and may be a useful tool to study the molecular pathology of, and development of therapeutic drugs for gastric cancer.

References

1. Nusse R. Wnt signaling in disease and in development. *Cell Res* 2005;15:28-32.
2. Oshima M, Oshima H, Kitagawa K, Taketo MM. Loss of Apc heterozygosity and abnormal tissue building in nascent intestinal polyps in mice carrying a truncated Apc gene. *Proc Natl Acad Sci USA* 1995;92:4482-4486.
3. Harada N, Tamai Y, Ishikawa T, Sauer B, Takaku K, Oshima M, Taketo MM. Intestinal polyposis in mice with a dominant stable mutation of the β -catenin gene. *EMBO J* 1999;18:5931-5942.
4. Clements WM, Wang J, Sarnaik A, Kim OJ, MacDonald J, Fenoglio-Preiser C, Groden J, Lowy AM. β -Catenin mutation is a frequent cause of Wnt pathway activation in gastric cancer. *Cancer Res* 2002;62:3503-3506.
5. Correa P. *Helicobacter pylori* infection and gastric cancer. *Cancer Epidemiol Biomarkers Prev* 2003;12:238-241.
6. Oshima H, Oshima M, Inaba K, Taketo MM. Hyperplastic gastric tumors induced by activated macrophages in COX-2/mPGES-1 transgenic mice. *EMBO J* 2004;23:1669-1678.
7. Murakami M, Naraba H, Tanioka T, Semmyo N, Nakatani Y, Kojima F, Ikeda T, Fueki M, Ueno A, Oh-ishi S, Kudo I. Regulation of prostaglandin E₂ biosynthesis by inducible membrane-associated prostaglandin E₂ synthase that acts in concert with cyclooxygenase-2. *J Biol Chem* 2000;275:32783-32792.

8. Yoshimatsu K, Golijanin D, Paty PB, Soslow RA, Jakobsson PJ, DeLellis RA, Subbaramaiah K, Dannenberg, AJ. Inducible microsomal prostaglandin E synthase is overexpressed in colorectal adenomas and cancer. *Clin Cancer Res* 2001;7:3971-3976.
9. Gupta RA, DuBois RN. Colorectal cancer prevention and treatment by inhibition of cyclooxygenase-2. *Nat Rev Cancer* 2001;1:11-21.
10. Saukkonen K, Tomasetto C, Narko K, Rio MC, Ristimaki A. Cyclooxygenase-2 expression and effect of celecoxib in gastric adenomas of trefoil factor 1-deficient mice. *Cancer Res* 2003;63:3032-3036.
11. Oshima M, Dinchuk JE, Kargman SL, Oshima H, Hancock B, Kwong E, Trzaskos JM, Evans JF, Taketo MM. Suppression of intestinal polyposis in *Apc*^{A716} knockout mice by inhibition of cyclooxygenase 2 (COX-2). *Cell* 1996;87:803-809.
12. Sonoshita M, Takaku K, Sasaki N, Sugimoto Y, Ushikubi F, Narumiya S, Oshima M, Taketo MM. Acceleration of intestinal polyposis through prostaglandin receptor EP2 in *Apc*^{A716} knockout mice. *Nat Med* 2001;7:1048-1051.
13. Pai R, Soreghan B, Szabo IL, Pavelka M, Baatar D, Tarnawski AS. Prostaglandin E2 transactivate EGF receptor: A novel mechanism for promoting colon cancer growth and gastrointestinal hypertrophy. *Nat Med* 2002;8:289-293.
14. Korinek V, Barker N, Moerer P, van Donselaar E, Huls G, Peters PJ, Clevers H. Depletion of epithelial stem-cell compartments in the small intestine of mice lacking

Tcf-4. *Nat Genet* 1998;19:1-5.

15. Pinto D, Gregorieff A, Begthel H, Clevers H. Canonical Wnt signals are essential for homeostasis of the intestinal epithelium. *Genes Dev* 2003;17:1709-1713.
16. Karam SM, Leblond CP. Dynamics of epithelial cells in the corpus of the mouse stomach. I. Identification of proliferative cell types and pinpointing of the stem cells. *Anat Rec* 1993;236:236-279.
17. Oshima M, Oshima H, Matsunaga A, Taketo MM. Hyperplastic gastric tumors with spasmolytic polypeptide-expressing metaplasia (SPEM) caused by TNF- α -dependent inflammation in COX-2/mPGES-1 transgenic mice. *Cancer Res* 2005;65:9147-9151.
18. Schmidt PH, Lee JR, Joshi V, Playford RJ, Poulsom R, Wright NA, Goldenring JR. Identification of a metaplastic cell lineage associated with human gastric adenocarcinoma. *Lab Invest* 1999;79:639-646.
19. Pull SL, Doherty JM, Mills JC, Gordon JI, Stappenbeck TS. Activated macrophages are an adaptive element of the colonic epithelial progenitor niche necessary for regenerative responses to injury. *Proc Natl Acad Sci USA* 2005;102:99-104.
20. Coussens LM, Werb Z. Inflammation and cancer. *Nature* 2002;420:860-867.
21. Seno H, Oshima M, Ishikawa T, Oshima H, Takaku K, Chiba T, Narumiya S, Taketo MM. Cyclooxygenase-2 and prostaglandin E₂ receptor EP₂-dependent angiogenesis in *Apc*¹⁷¹⁶ mouse intestinal polyps. *Cancer Res* 2002;62:506-511.
22. Halldorsdottir AM, Sigurdardottir M, Jonasson JG, Oddsdottir M, Magnusson J, Lee

JR, Goldenring JR. Spasmolytic polypeptide-expressing metaplasia (SPEM)

associated with gastric cancer in Iceland. *Dig Dis Sci* 200;48:431-41.

23. Wang D, Wang H, Shi Q, Katkuri S, Walhi W, Desvergne B, Das SK, Dey SK, DuBois RN. Prostaglandin E₂ promotes colorectal adenoma growth via transactivation of the nuclear peroxisome proliferator-activated receptor δ . *Cancer Cell* 2004;6:285-295.
24. Castellone MD, Teramoto H, Williams BO, Druey KM, Gutkind JS. Prostaglandin E₂ promotes colon cancer cell growth through a G_S-Axin- β -catenin signaling axis. *Science* 2005;310:1504-1510.

Figure Legends

Figure 1

Nuclear localization of β -catenin in human gastric cancer. Representative histological sections (H&E) of intestinal-type (A) and diffuse type (D) gastric cancer.

Immunostaining for unphosphorylated β -catenin in sections adjoining (A) and (D) are shown in (B) and (E), respectively. The total β -catenin staining in the adjacent normal tissues of the same patients is shown in (C) and (F). Insets show higher magnifications where β -catenin is localized in the nuclei of intestinal-type and diffuse type gastric cancer cells, while it is found in the basolateral membrane of the adjacent normal epithelial cells. Scale bars in (A-F) are 200 μ m. (G) Numbers and percentages of nuclear β -catenin-positive gastric cancer cases.

Figure 2

Generation of *K19-Wnt1* transgenic mice. (A) Construction of the transgenic vector. The artificial intron between the K19 promoter and *Wnt1* cDNA is shown as a V-shape. *Wnt1* cDNA and SV40 poly(A) fragments are shown as gray and black boxes, respectively. Pm, *PmeI*; N, *NcoI*; B, *BamHI*; Xb, *XbaI*. (B) RT-PCR for *Wnt1* mRNA in the gastric mucosa of the wild-type, *K19-C2mE*, *K19-Wnt1* and *K19-Wnt1/C2mE* transgenic mice. *K19-C2mE* and *K19-Wnt1* transgenic mice. GAPDH was used as an internal control. (C) Immunoblotting of the gastric extracts from *K19-Wnt1*

transgenic lines (#1 through #5) for total (*top*) and unphosphorylated (activated form) β -catenin (*middle*) compared with that from wild-type mice (*WT*) and *Apc*^{A716} mouse normal intestine (*N*) and polyps (*P*). β -Actin was used as an internal control (*bottom*). Note that all *K19-Wnt 1* lines (#1 through #5) show an increased level of the unphosphorylated β -catenin compared with that of wild-type mice. Two lines (#1 and #2) show comparable levels to that in the *Apc*^{A716} mouse intestinal polyps. (*D*) Immunoblotting for COX-2 in the glandular stomach of the respective transgenic strains.

Figure 3

Gastric epithelial differentiation was suppressed by Wnt signaling. (*A*) H&E staining of the isthmus of the glandular stomach, (*B*) *in situ* hybridization for TFF2, and (*C*) immunostaining for β -catenin using serial sections of (*A*). The arrowheads indicate isthmal small cells with TFF2 expression and β -catenin accumulation (progenitor cells). Scale bars in (*A-C*) are 100 μ m. (*D*) TFF2-expressing cells (asterisks) in the glandular stomach of the wild-type (*left*) and *K19-Wnt1* (*right*) mice (*in situ* hybridization). Histogram shows the mean number of TFF2-positive cells per gland (mean \pm s.d.). (*E*) Cells incorporated BrdU (asterisks) with 30 minute-labeling in the glandular stomach of the wild-type (*left*) and *K19-Wnt1* (*right*) mice (immunostaining). Histogram shows the BrdU labeling index (mean \pm s.d.). (*F*) Cells labeled with Ki-67

(asterisks) in the glandular stomach of the wild-type (*left*) and *K19-Wnt1* (*right*) mice (immunostaining). Histogram shows the Ki-67 labeling index (mean \pm s.d.). Scale bars in (*D-F*) are 200 μ m. Note that the numbers of TFF2-positive cells, BrdU labeled cells, and Ki-67-stained cells all increased significantly in the *K19-Wnt1* mouse glandular stomach compared with those in the wild-type mice.

Figure 4

Small preneoplastic lesions in the glandular stomach of *K19-Wnt1* mice at 7 weeks (*B*) and 18 weeks of age (*C*), and control wild-type mice at 18 weeks of age (*A*). Arrows indicate small preneoplastic lesions. Toluidine blue staining. Scale bars in (*A-C*) are 0.5 mm. (*D*) H&E staining of the preneoplastic lesions, (*E*) Ki-67 and (*F*) β -catenin immunostaining using serial sections of (*D*). The open arrowheads in (*D-F*) indicate small undifferentiated epithelial cells with an increased proliferation and β -catenin accumulation. Inset in (*F*) shows a higher magnification of β -catenin accumulated cells. Scale bars in (*D-F*) are 100 μ m.

Figure 5

Gastric tumors in *K19-Wnt1/C2mE* mice. Macroscopic photographs (*top*) and H&E staining (*bottom*) of the glandular stomach of the wild-type (*A*), *K19-Wnt1/C2mE* (*B*), *K19-Wnt1* (*C*) and *K19-C2mE* (*D*) mice at 30 weeks of age. Arrowheads (white in *top*

and black in *bottom* panels) indicate the border between the glandular stomach and forestomach. Small arrows in (C) point to the preneoplastic lesions. Large arrows in (A) indicate dysplastic tumors with hyperemia in the *K19-Wnt1/C2mE* stomach. No such tumors were found in either of the simple transgenic strains. Scale bars in (A-D, *bottom*) are 2 mm. (E) Histology of the *K19-Wnt1/C2mE* gastric tumors (H&E). Serial sections of (E), immunostained for β -catenin (F) and Ki-67 (G). Arrows in (E and F) indicate dysplastic epithelial cells with the nuclear accumulation of β -catenin. The scale bars in (E-G) are 100 μ m. (H) *in situ* hybridization for TFF2 to detect SPEM cells (arrows) adjacent to the dysplastic tumors in the *K19-Wnt1/C2mE* mice at 30 weeks of age. (I) The arrowheads point to the invasion of tumor epithelial cells into the smooth muscle layers (H&E). Scale bar in (I) is 200 μ m. (J) The number of mice with invasive tumors in the *K19-Wnt1/C2mE* mice at 10, 20, 30 and 50 weeks of age. (K) Incidence of dysplastic tumors in the respective mouse strains older than 20 weeks of age.

Figure 6

Immunostaining for macrophages using F4/80 antibody in the wild-type mouse stomach (A), *K19-Wnt1/C2mE* tumor (B) and *K19-Wnt1* preneoplastic lesion (C). Heavy macrophage accumulation was found in the *K19-Wnt1/C2mE* mouse tumor. The arrows in (A) indicate sparsely scattered tissue macrophages in the normal stomach. The arrowheads in (C) indicate the macrophages accumulated in the

preneoplastic lesion. Scale bars in (A-C) are 100 μm . Immunostaining for capillary vessels using anti-vWF antibody in the *K19-Wnt1* stomach (D) and *K19-Wnt1/C2mE* tumor (E). Scale bars in (D, E) are 100 μm . (F) Relative microvessel density (MVD) to the wild-type level is shown (mean \pm s.d.). *, $P < 0.05$, versus wild-type mice. +, $P < 0.05$, versus *K19-Wnt1* mice.

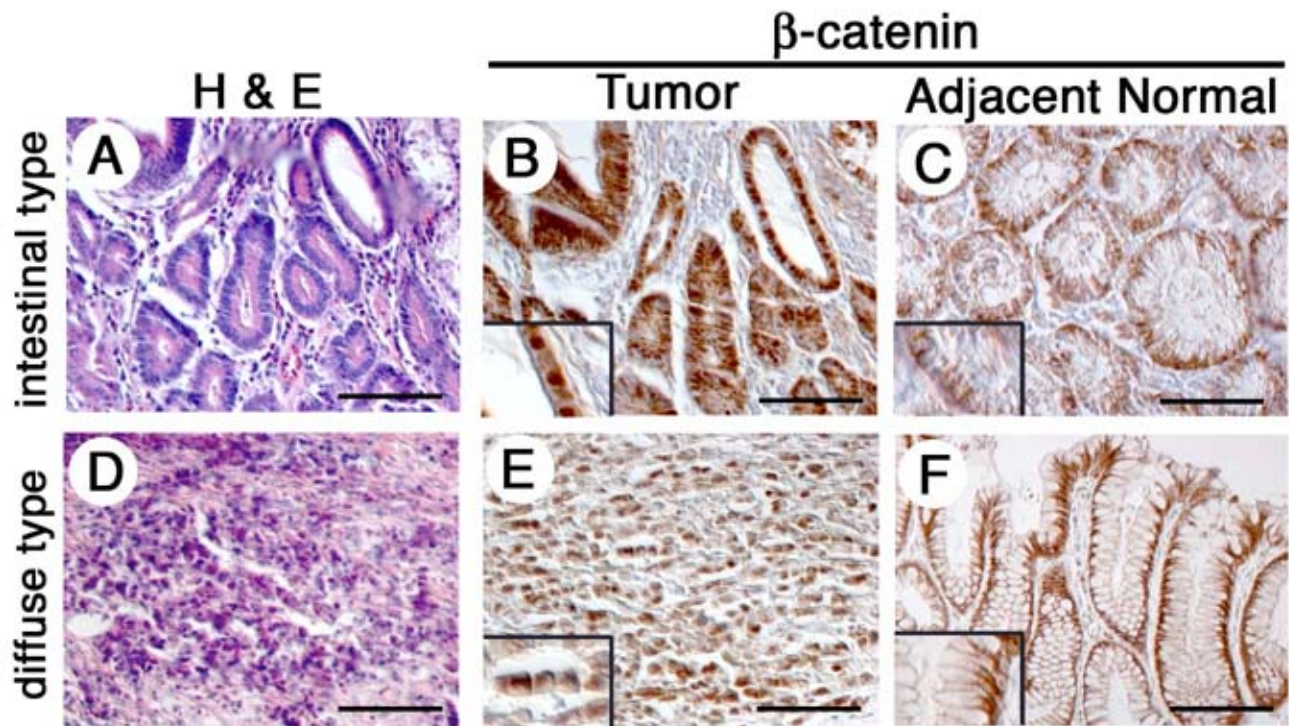
Figure 7

Chronological changes in gastric tumorigenesis in the *K19-Wnt1/C2mE* mice (A-H) and *K19-C2mE* mice (I-P) at 5, 10, 20 and 50 weeks of age. H&E staining (A-D and I-L), and Alcian blue staining at pH2.5 of the serial sections (E-H and M-P). Alcian blue staining in the wild-type mouse stomach (WT) is also shown (E: right). The arrows indicate Alcian blue-positive metaplastic mucous cells. Arrowhead in (E, right) indicates Alcian blue-positive normal mucous neck cells. The dotted lines in (B, C, F, and G) indicate the border between the metaplastic and dysplastic (Dys) regions. Scale bars are 100 μm . Both strains show mucous metaplasia after 5 weeks of age. However, dysplastic epithelial cells are found only in the *K19-Wnt1/C2mE* stomach after 10 weeks of age. Dysplastic epithelial cells predominate the tumor tissues of the *K19-Wnt1/C2mE* mice at 20 and 50 weeks of age.

Figure 8

The BrdU labeling index in the glandular stomach of the wild-type (green), *K19-C2mE* (gray) and *K19-Wnt1/C2mE* (black) mice at 5, 10, 20, and 50 weeks of age (mean \pm s.d.). *, $P < 0.05$, versus wild-type mice. +, $P < 0.05$, versus *K19-C2mE* mice. The BrdU indices in the *K19-C2mE* and *K19-Wnt1/C2mE* glandular stomach are significantly higher than those in the wild-type mice. *K19-Wnt1/C2mE* mice show even higher proliferation rate than that in the *K19-C2mE* mice at 20 and 50 weeks of age.

Figure 1



G

Histology	Nuclear β -catenin (%)	Total
Intestinal type	24 (51)	47
Diffuse type	19 (58)	33
Total	43 (54)	80

Figure 2

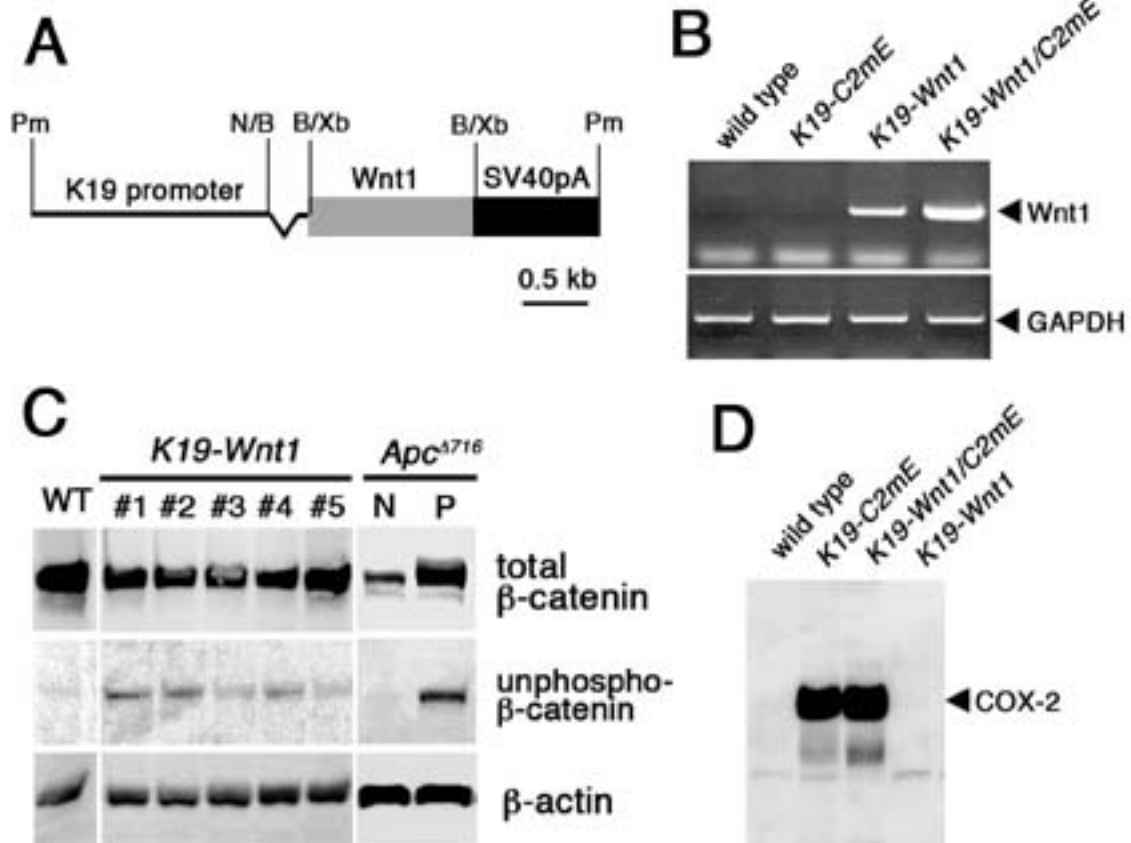


Figure 3

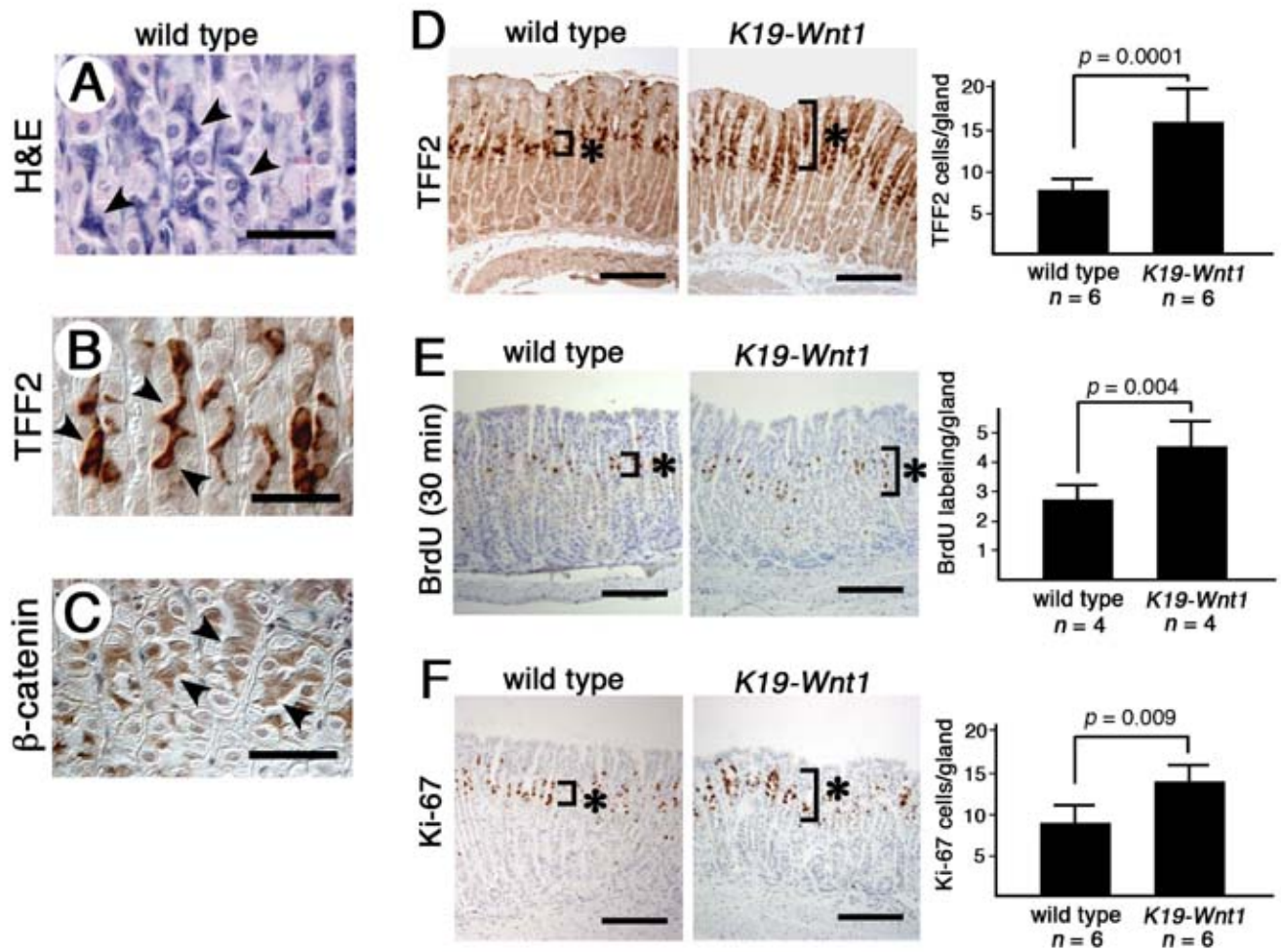


Figure 4

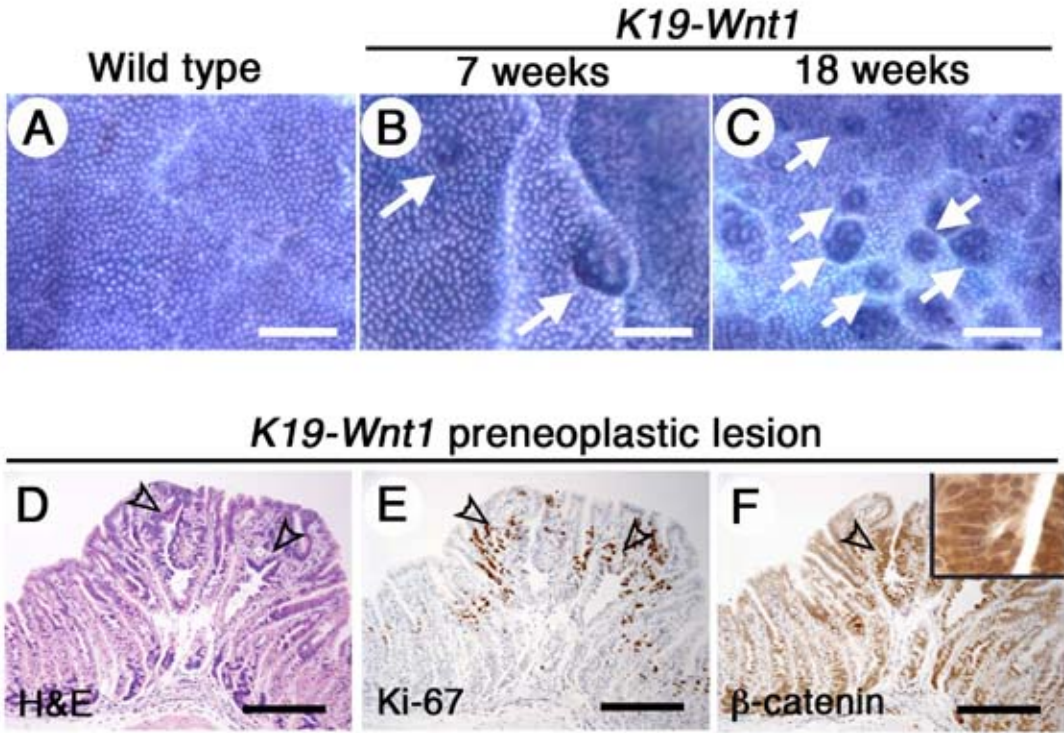
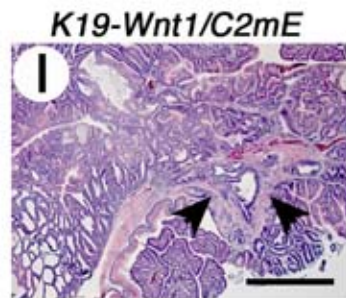
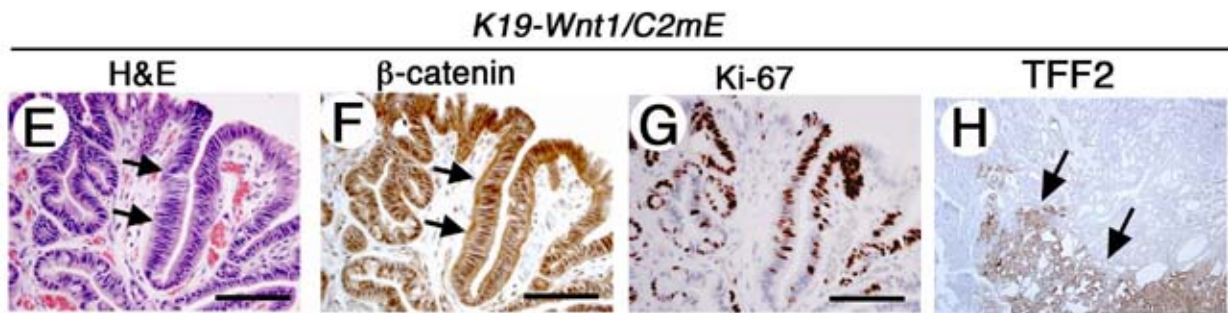
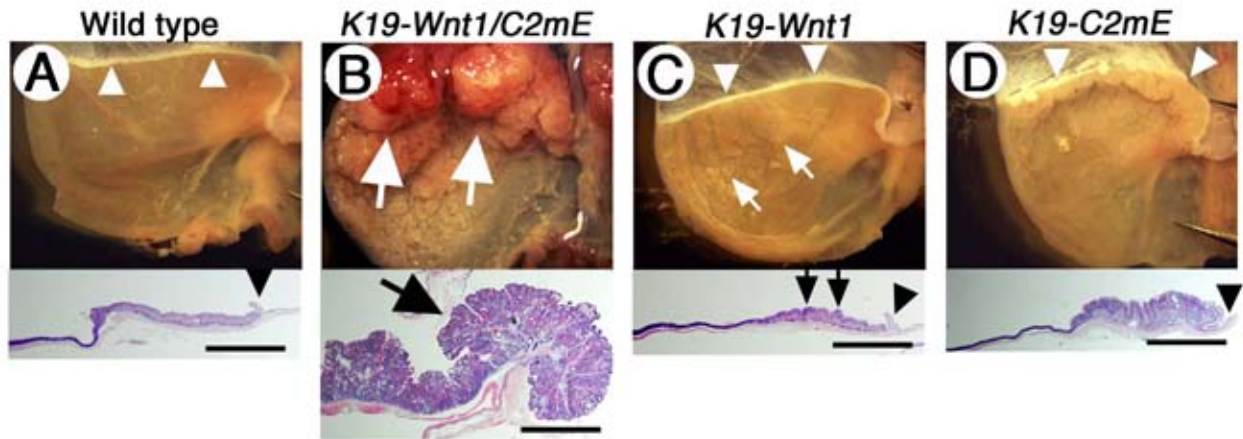


Figure 5



J

Age (w)	invasion/total (%)
10	0 / 3 (0)
20	1 / 2 (50)
30	6 / 8 (75)
50	4 / 4 (100)

K

Genotype	Dysplastic tumor (%)
<i>K19-C2mE</i>	0 / 20 (0)
<i>K19-Wnt1/C2mE</i>	14 / 14 (100)
<i>K19-Wnt1</i>	0 / 14 (0)
Wild type	0 / 13 (0)

Figure 6

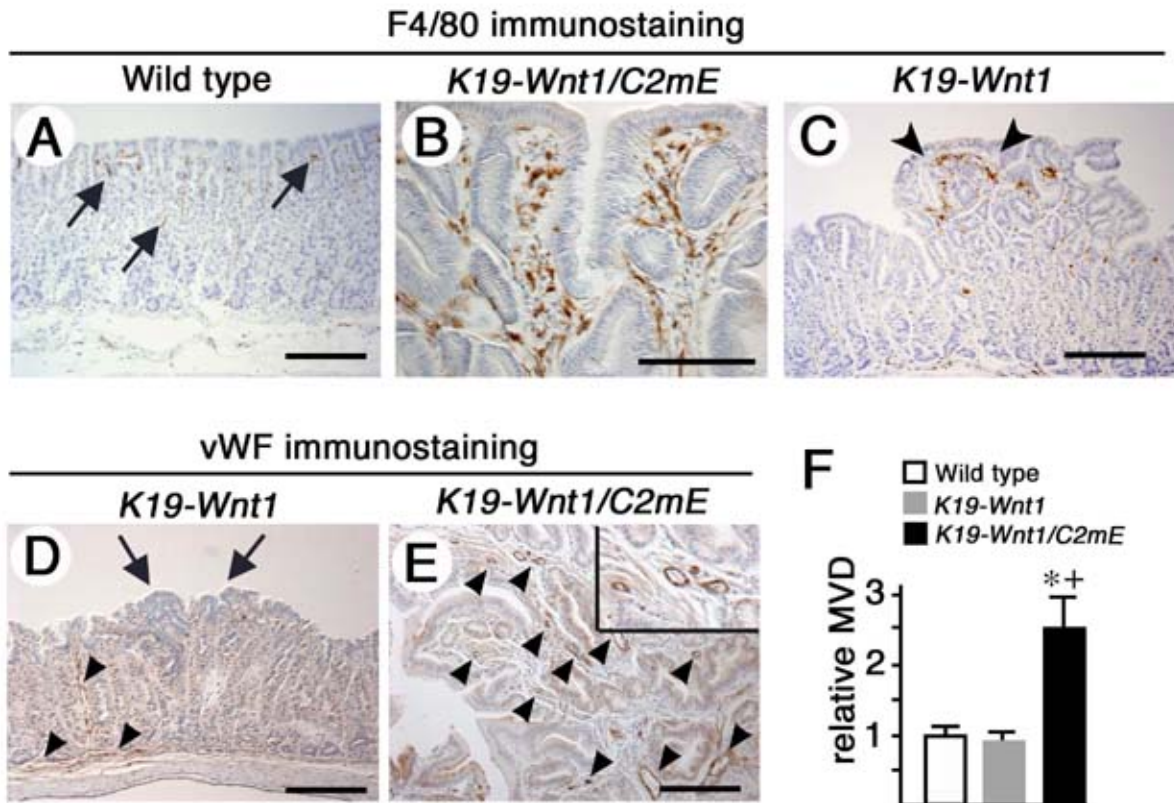


Figure 7

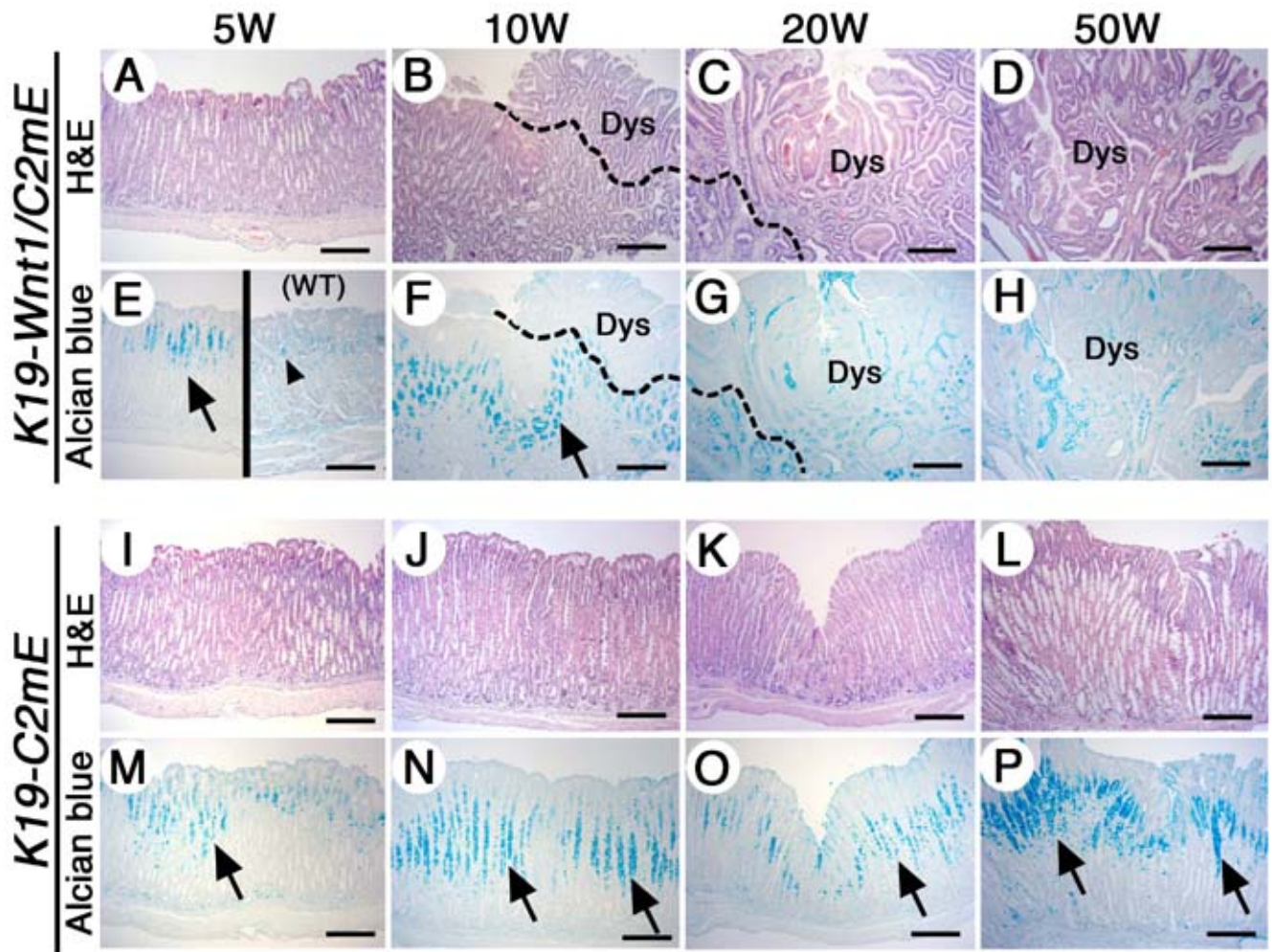


Figure 8

